Original Article

IL23R as an indicator of immune infiltration and poor prognosis in intrahepatic cholangiocarcinoma: a bioinformatics analysis

Lin-Ting Zhang[1,2#], Yi-Fan Yang[1,3#], Xiao-Ming Chen[3], Shu-Bin Wang[2], Gang-Ling Tong[1,2]

[1]Shantou University Medical College, Shantou, China; [2]Department of Oncology, Peking University Shenzhen Hospital, Shenzhen Key Laboratory of Gastrointestinal Cancer Translational Research, Cancer Institute of Shenzhen-Peking University-Hong Kong University of Science and Technology (PKU-HKUST) Medical Center, Shenzhen, China; [3]Department of Interventional Radiology, Guangdong Provincial People's Hospital, Guangdong Academy of Medical Sciences, Guangzhou, China

Contributions: (I) Conception and design: LT Zhang, YF Yang; (II) Administrative support: XM Chen, SB Wang, GL Tong; (III) Provision of study materials or patients: LT Zhang, YF Yang; (IV) Collection and assembly of data: LT Zhang, YF Yang; (V) Data analysis and interpretation: LT Zhang, YF Yang; (VI) Manuscript writing: All authors; (VII) Final approval of manuscript: All authors.

[#]These authors contributed equally to this work as co-first authors.

Correspondence to: Gang-Ling Tong, MD. Shantou University Medical College, Shantou, China; Department of Oncology, Peking University Shenzhen Hospital, Shenzhen Key Laboratory of Gastrointestinal Cancer Translational Research, Cancer Institute of Shenzhen-Peking University-Hong Kong University of Science and Technology (PKU-HKUST) Medical Center, 1120 Lianhua Road, Futian, Shenzhen 518036, China. Email: tgl221747@sohu.com.

Background: Although the incidence of intrahepatic cholangiocarcinoma (CHOL) is low, the prognosis is very poor. The expression level of interleukin 23 receptor (*IL23R*) is linked to the occurrence and development of cancers. This study aimed to identify the role of *IL23R* in CHOL using bioinformatics tools and experimental validation.

Methods: Circular RNA (circRNA), microRNA (miRNA), and messenger RNA (mRNA) datasets were obtained from the Gene Expression Omnibus (GEO) database, and R software was used for data analysis and visualization. Gene Ontology (GO) and Kyoto Encyclopedia of Genes and Genomes (KEGG) were used to conduct functional enrichment analysis, which was verified with gene set enrichment analysis software. Clinical data were obtained from The Cancer Genome Atlas (TCGA), and survival analyses were performed using the DriverDBv3 database and the Gene Expression Profiling Interactive Analysis website. The TIMER2.0 database provided us for immune cell infiltration analysis results of *IL23R*. Real-time quantitative polymerase chain reaction (RT-qPCR) was used for *IL23R* expression verification.

Results: Differentially expressed (DE) mRNAs were enriched in phosphoinositide 3-kinase-serine/threonine kinase signaling pathway, immune-related tumor microenvironment (TME), and amino acid metabolism, etc. In addition, expression of *IL23R* was associated with immune infiltration-related cells. Furthermore, a circRNA-miRNA-*IL23R* network and a *IL23R* protein-protein interaction network were established. Most importantly, *IL23R*, as a prognostic gene, was found to have a low expression in CHOL.

Conclusions: A circRNA-miRNA-*IL23R* network was identified, and it was found that *IL23R* may be a prognostic and immune-related biomarker in CHOL, which is worthy of further exploration.

Keywords: Intrahepatic cholangiocarcinoma (CHOL); interleukin 23 receptor (*IL23R*); bioinformatics; biomarker; prognosis

Submitted Mar 18, 2023. Accepted for publication Sep 01, 2023. Published online Oct 16, 2023.
doi: 10.21037/tcr-23-455
View this article at: https://dx.doi.org/10.21037/tcr-23-455

Introduction

Originating from biliary system, cholangiocarcinoma (CCA) is the second most common primary liver tumor (1). CCA can be divided into 3 types: intrahepatic CCA (CHOL), perihilar CCA, and distal CCA (1). Among these, CHOL is the least common type of CCA (2,3). Although the incidence of CHOL at only 10–15% is very low compared to, for example, hepatocellular carcinoma, its prognosis is very poor (4,5). Due the concealed clinical features, difficult diagnosis, and limited treatment strategy for CHOL, the mortality rate of CHOL is increasing worldwide (6). Therefore, timely diagnosis and treatment is particularly important. Moreover, an effective staging system of CHOL is essential to providing prognostic information and guiding therapy. Unfortunately, most existing staging systems are deficient in treatment selection and lack prognostic accuracy (3). Therefore, reliable prognostic indicators are urgently needed to enable optimal treatment allocation and prediction.

Interleukin 23 receptor (*IL23R*) is the receptor for IL-23 binding, and IL-23 binds to receptors composed of IL-12R β2 and *IL23R* (7). Studies have revealed that *IL23R* performs an essential role in tumorigenesis, especially in the immune tumor microenvironment (TME) (8-10). It was reported that intratumoral regulatory T cells (Tregs) became unstable due to antibody-mediated *IL23R* blockade, and this process could enhance immunotherapy (10). In studies related to the treatment of laryngeal cancer, *IL23R* was demonstrated to be a marker of the immunoediting process, as IL-23/*IL23R* can reduce the activation of signal transducer and activator of transcription 3 (STAT3), providing potential immunotherapy in the preservation of laryngeal function and improving survival (9). Research also indicates that *IL23R* is related to the prognosis of gastric cancer and non-small cell lung carcinoma (11,12). *IL23R* is also associated with other immune-related diseases, such as ankylosing spondylitis, rheumatoid arthritis, psoriasis, and inflammatory bowel disease (13-15). In a recent study, it was reported that a higher baseline level of IL-23 could improve the clinical results of atezolizumab combined with cobimetinib in the treatment of advanced biliary tract cancers (16). However, no studies have focused on the role of *IL23R* in CHOL or its relation to the immune TME.

Circular RNA (circRNA) as a competitive endogenous regulator, plays a key role in the occurrence and development of cancer. circRNA is formed by reverse splicing, which has the characteristics of covalent loop closure, high conservatism, and stability (17,18). Multiple studies have shown that circRNAs are abnormally expressed in CHOL and regulate the progression of tumor cells. For example, the low expression of circRTN4IP1 was found to inhibit the proliferation of CHOL through the miR-541-5p-HIF1A axis (19). circHMGCS1-016 was shown to be involved in CHOL development and immune tolerance through the miR-1236-3p-CD73 and GAL-8 axis (20). Furthermore, circACTN4 was shown to activate FZD7 transcription through miR-424-5p and its interaction with YBX1 to promote CHOL proliferation and metastasis (21). Therefore, greater attention should be paid to the role of circRNA in CHOL and to the regulatory network of competing endogenous RNA (ceRNA) in CHOL. However, no research concerning the role of the circRNA-miRNA-*IL23R* regulatory network in CHOL exists.

For patients with CHOL, the prognosis is often poor and the treatment is inadequate. The existing literature that higher baseline level of IL-23 could improve the clinical outcomes in the treatment of advanced biliary tract cancers. *IL23R* as the receptor of IL-23 is underexplored. In addition, research indicates that some circRNAs are abnormally expressed in CHOL and may affect its progression. Further study on the role of circRNAs in CHOL may provide improved guidance for the diagnosis and treatment of patients with CHOL. In this study, we thus aimed to characterize the expression level of *IL23R* using bioinformatics methods and to explore the relationship between *IL23R* and circRNA. We found that the expression level of *IL23R* was related to the overall survival (OS) of patients with CHOL and observed a relationship between *IL23R* and the infiltration level of immune cells. We hope that our findings offer insights into the emergence and progression of CHOL and aid in identifying new therapeutic targets for effective treatment (*Figure 1*). We present this article in accordance with the

Highlight box

Key findings

- Interleukin 23 receptor (*IL23R*) may be a prognostic and immune-related biomarker in intrahepatic cholangiocarcinoma (CHOL).

What is known and what is new?

- CHOL has a low incidence but a poor prognosis.
- *IL23R* can predict the prognosis of CHOL.

What is the implication, and what should change now?

- The role of *IL23R* in CHOL needs further study.

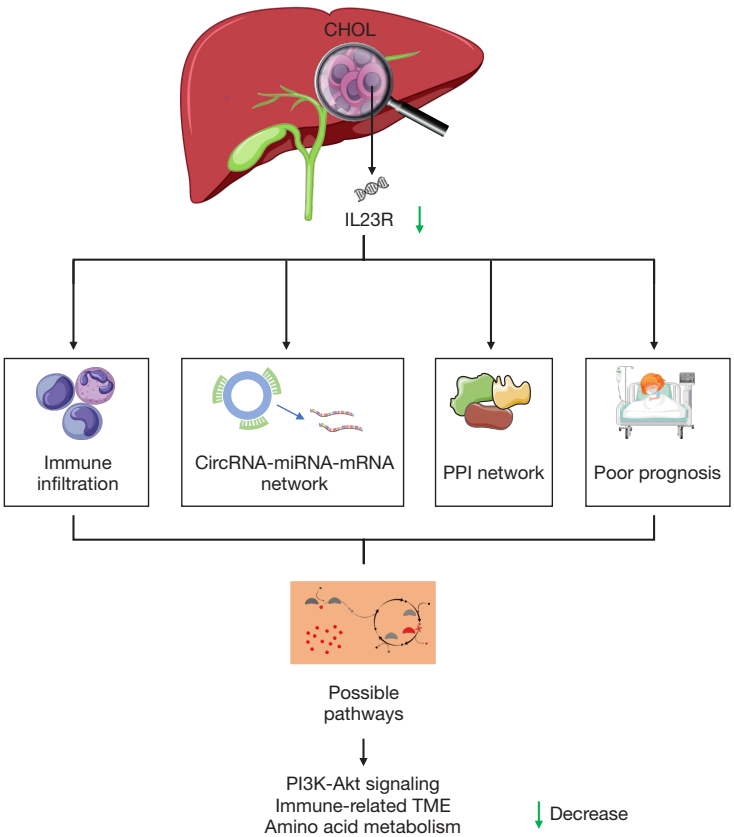

Figure 1 *IL23R* as an immune infiltration and prognostic signature of poor prognosis in intrahepatic cholangiocarcinoma. The image elements are from Vecteezx (http://www.vecteezy.com/) and SMART SERVIER (https://smart.servier.com/). CHOL, intrahepatic cholangiocarcinoma; *IL23R*, interleukin 23 receptor; circRNA, circular RNA; miRNA, microRNA; mRNA, messenger RNA; PPI, protein-protein interaction; PI3K, phosphoinositide 3-kinase; Akt, serine/threonine kinase; TME, tumor microenvironment.

TRIPOD reporting checklist (available at https://tcr.amegroups.com/article/view/10.21037/tcr-23-455/rc).

Methods

Data acquisition and preprocessing

Microarray RNA expression data were obtained from Gene Expression Omnibus (GEO) database (https://www.ncbi.nlm.nih.gov/geo/; RRID: SCR_005012), specifically, the GSE181523, GSE32957, and GSE61850 datasets. The GSE181523 dataset included 7 CHOL samples and 7 nontumor tissue samples, the GSE32957 dataset included 16 CHOL samples and 5 nontumor tissue samples, and the GSE61850 dataset included 5 CHOL samples and 5 adjacent normal tissue samples. Differential expression analyses were performed using R version 4.1.2. (The R Foundation for Statistical Computing; RRID: SCR_001905), specifically, the "limma", "pheatmap", and "ggplot2" package. The $|\log_2$ fold change (FC)$|$ >1 and adjusted P value <0.05 were set as thresholds. We used the CircBank database (http://www.circbank.cn/index.html) (22) to identify the microRNA (miRNA) response elements (MREs). Targetscan (https://www.targetscan.org/vert_80/; RRID: SCR_010845) (23) was used to obtain the target genes. The intersection of MREs and differentially expressed (DE) miRNAs and the intersection of DE messenger RNA (DEmRNA) and the miRNA target gene (tar-DEmRNA) were obtained using an online Venn diagram tool (http://bioinformatics.psb.ugent.be/webtools/Venn/). The circRNA-miRNA-mRNA network was established with Cytoscape v. 3.9.0 software (RRID: SCR_003032). The data for OS and disease-free survival (DFS) of patients with CHOL in The Cancer Genome Atlas (TCGA) were obtained from the University of California, Santa Cruz (UCSC) Xena website (https://xenabrowser.

Table 1 Clinical characteristics of 32 patients with intrahepatic cholangiocarcinoma from The Cancer Genome Atlas

Variables	Values
Age (years)	63 [29–82]
Gender	
Male	14 (43.8)
Female	18 (56.3)
Race	
White	27 (84.4)
Black or African American	2 (6.3)
Asian	3 (9.4)
Ethnicity	
Hispanic or Latino	2 (6.3)
Not Hispanic or Latino	30 (93.8)
TNM stage	
T	
T1	17 (53.1)
T2	5 (15.6)
T2a	2 (6.3)
T2b	3 (9.4)
T3	5 (15.6)
N	
N0	24 (75.0)
N1	4 (12.5)
NX	4 (12.5)
M	
M0	26 (81.3)
M1	3 (9.4)
MX	3 (9.4)
Stage	
Stage I	17 (53.1)
Stage II	10 (31.3)
Stage IV	5 (15.6)
Site of resection or biopsy	
Intrahepatic bile duct	31 (96.9)
Liver	1 (3.1)
Tissue or organ of origin	
Intrahepatic bile duct	31 (96.9)
Liver	1 (3.1)
Treatment type	
Pharmaceutical therapy	17 (53.1)
Radiation therapy	15 (46.9)

Data are presented as n (%) or median [range]. TNM, tumor, node, metastasis.

Table 2 Clinical characteristics of 8 normal samples from The Cancer Genome Atlas

Variables	Values
Age (years)	73 [52–82]
Gender	
Male	5 (62.5)
Female	3 (37.5)
Race	
White	8 (100.0)
Black or African American	0
Asian	0
Ethnicity	
Hispanic or Latino	0
Not Hispanic or Latino	8 (100.0)
Site of resection or biopsy	
Intrahepatic bile duct	8 (100.0)
Liver	0
Tissue or organ of origin	
Intrahepatic bile duct	8 (100.0)
Liver	0

Data are presented as n (%) or median [range].

net/datapages/; RRID: SCR_018938). The demographic information related to the patients with CHOL from TCGA is provided in *Table 1*. Patients with CHOL range in age from 29 to 82 years old. For comparison, the information of normal samples from TCGA is provided in *Table 2*. The normal samples ranged in age from 52 to

82 years old. This study was conducted in accordance with the Declaration of Helsinki (as revised in 2013) and was approved by Ethics Committee of Guangdong Provincial People's Hospital (No. KY-Q-2022-321-01). Written informed consent for participation was not required for this study in accordance with the national legislation and the institutional requirements.

Functional enrichment analysis

Gene Ontology (GO) (RRID: SCR_002811) and Kyoto Encyclopedia of Genes and Genomes (KEGG) (RRID: SCR_012773) were used to conduct functional enrichment analyses (24,25) via The Database for Annotation, Visualization and Integrated Discovery (DAVID) analysis tool (https://david.ncifcrf.gov/home.jsp; RRID: SCR_001881) (26,27). GO annotations included cellular component, molecular function, and biological process. A false discovery rate (FDR) <0.05 was set as the statistical significance threshold. In addition, gene set enrichment analysis (GSEA) (http://www.gsea-msigdb.org/gsea/index.jsp; RRID: SCR_003199) software (28-31) was used to verify the functional enrichment of the tar-DEmRNAs.

Survival analysis

The DriverDBv3 (http://driverdb.tms.cmu.edu.tw/; RRID: SCR_007736) database and Gene Expression Profiling Interactive Analysis (GEPIA) website (http://gepia.cancer-pku.cn/index.html; RRID: SCR_018294) were used to perform survival analyses. DriverDBv3 is a database for human cancer driver gene research (32), while GEPIA is a web server for analyzing the RNA sequencing expression data (33). R version 4.1.2. and GraphPad Prism v. 8.0 (GraphPad Software; RRID: SCR_002798) were used to verify the relationship between *IL23R* and OS or DFS using the log-rank (Mantel-Cox) test. A P value <0.05 indicated statistical significance.

Immune cell infiltration analysis

The Venn diagram online tool was used to identify the intersection of tar-DEmRNA genes and immune-related genes from the Immunology Database and Analysis Portal (ImmPort) database (https://www.immport.org/home; RRID: SCR_012804) (34). Immune infiltrate abundance were acquired from TIMER2.0 (http://timer.comp-genomics.org/) via multiple immune deconvolution methods (35-37), including TIMER, EPIC, MCP-COUNTER, CIBERSORT, CIBERSORT-ABS, QUANTISEQ, XCELL, and TIDE methods. The immune cells included $CD4^+$ T cells, $CD8^+$ T cells, Tregs, B cells, neutrophils, monocytes, macrophages, dendritic cells (DCs), natural killer (NK) cells, mast cells, cancer-associated fibroblasts, common lymphoid progenitors, common myeloid progenitors, endothelial cells, eosinophils, granulocyte-monocyte progenitors, hematopoietic stem cells, follicular helper T cells, gamma delta T cells, NK T cells, and myeloid-derived suppressor cells (MDSCs).

Real-time quantitative polymerase chain reaction (RT-qPCR)

Total *IL23R* RNA was extracted using TRIzol (Invitrogen, Thermo Fisher Scientific, Carlsbad, CA, USA) and reverse transcribed into complement DNA (cDNA) according to instruction of the Transcriptor cDNA Synth Kit (Roche, Basel, Swiss). RT-qPCR was conducted using the SYBR Green PCR kit (Qiagen, Hilden, Germany) and according to the manufacturer's instruction. The relative gene expression changes were analyzed with the $2^{-\Delta\Delta Ct}$ method. The forward primer for *IL23R* was 5'-GCTCGGATTTGGTATAAAGG-3', and the reverse primer for *IL23R* was 5'-ACTTGGTATCTATGTAGGTAGG-3'. The forward primer for β-actin was 5'-TCCCTGGAGAAGAGCTACGA-3', and the reverse primer for β-actin was 5'-AGCACTGTGTTGGCGTACAG-3'.

Statistical analysis

GraphPad Prism 8.0 and R version 4.1.2. were used to analyze and visualize the data. The Student's *t*-test was used to compare continuous variables between 2 groups. A P value <0.05 was considered statistically significant.

Results

Identification and preprocessing of DEcircRNA, DEmiRNA, and DEmRNA

To screen the DEcircRNA, DEmiRNA, and DEmRNA, we downloaded GSE181523, GSE32957, and GSE61850 datasets, consisting of 14 samples, 21 samples, and 10 samples, respectively. By using R software, we identified 69 upregulated and 104 downregulated circRNAs (*Figure 2A*,*2B*), 30 upregulated and 28 downregulated miRNAs were screened (*Figure 2C*,*2D*), and 2,234

upregulated and 2,203 downregulated mRNAs were confirmed (*Figure 2E,2F*). All DERNAs were visualized using volcano plots and heatmaps. The specific information of DEcircRNAs, DEmiRNAs, and DEmRNAs are shown in the online tables (available at https://cdn.amegroups.cn/static/public/10.21037tcr-23-455-1.pdf, https://cdn.amegroups.cn/static/public/10.21037tcr-23-455-2.pdf, and https://cdn.amegroups.cn/static/public/10.21037tcr-23-455-3.pdf).

After the DEcircRNAs were screened, we used CircBank to obtain the MREs that bond to circRNAs. After removing duplicate data, we identified 805 MREs, which are listed in the online table (available at https://cdn.amegroups.cn/static/public/10.21037tcr-23-455-4.pdf). hsa-miR-34c-5p, hsa-miR-516a-3p, hsa-miR-513a-3p, hsa-miR-1261, hsa-miR-512-3p, hsa-miR-199b-5p, and hsa-miR-1183 (*Figure 3A*), all of which are both MREs and DEmiRNAs, were screened with Venn diagram. We further used Targetscan to obtain the target genes (targetgene), and 1,864 mRNAs which were both target genes and DEmRNAs (tar-DEmRNA) (*Figure 3B*) were screened via Venn diagram.

Functional enrichment analysis of tar-DEmRNAs

We used the DAVID website to explore the functional enrichment of tar-DEmRNAs. There were 129 cellular component-related terms, 140 molecular function-related terms, and 456 biological process-related terms. We screened out 77 GO terms with statistical significance, including cytosol, plasma membrane, cytoplasm, integral component of membrane, and extracellular exosome, among others. There are 66 KEGG pathway terms, of which 22 were statistically significant, including metabolic pathways, pathways in cancer, phosphoinositide 3-kinase (PI3K)-serine/threonine kinase (Akt) signaling pathway, human papillomavirus infection, and focal adhesion, among others. *Figure 3C,3D* lists the top 10 most enriched terms, with their specific information being shown in the online table (available at https://cdn.amegroups.cn/static/public/10.21037tcr-23-455-5.pdf), including name of pathways, ID of pathways, number of enriched genes, proportion of enriched genes, P value, name of enriched genes. We verified the functional enrichment of tar-DEmRNAs using GSEA software, with the complete information being available in the online table (available at https://cdn.amegroups.cn/static/public/10.21037tcr-23-455-6.pdf). As shown in *Figure 3E* (28-31), according to KEGG analyses, CHOL samples, termed "carcinoma", were enriched in cancer pathway, cell cycle, ribosome, extracellular matrix (ECM)-receptor interaction, endocytosis, small-cell lung cancer, focal adhesion, gap junction, hypertrophic cardiomyopathy (HCM), oocyte meiosis, pathogenic *Escherichia coli* infection, and axon guidance as compared with healthy samples.

Relation of IL23R to CHOL immune infiltration abundance

We obtained the immune-related genes (imgene) using the ImmPort database. The Venn diagram online was then used to determine the intersection of tar-DEmRNA genes and imgenes, with 148 genes (im-tar-DEmRNA) being selected (*Figure 4A*). We found that among 148 im-tar-DEmRNAs, a low expression of *IL23R* was associated with poor prognosis in CHOL. We analyzed the relationship between *IL23R* expression and the immune cell infiltration in CHOL using TIMER2.0 database. As seen in *Figure 4B*, the expression of *IL23R* in CHOL was negatively correlated with the proportion of tumor cells (Rho =–0.418; P=1.12e–02) (35-37). *IL23R* expression had a positive correlation with the following immune cell types: B cells, according to the EPIC (Rho =0.398; P=1.77e–02), TIMER (Rho =0.363; P=3.19e–02) and XCELL (Rho =0.369; P=2.91e–02) methods; $CD4^+$ effector memory T cells, according to the XCELL (Rho =0.373; P=2.73e–02) method; $CD4^+$ T cells according to the EPIC (Rho =0.344; P=4.32e–02) method, myeloid DCs according to the MCPCOUNTER (Rho =0.347; P=4.08e–02) method; activated myeloid DCs according to the XCELL (Rho =0.386; P=2.20e–02) method; monocytes according to the CIBERSORT-ABS (Rho =0.463; P=5.11e–03) and CIBERSORT (Rho =0.432; P=9.48e–03) methods; M2 macrophages according to the CIBERSORT-ABS (Rho =0.356; P=3.59e–02) and QUANTISEQ (Rho =0.435; P=8.98e–03) methods; macrophages, according to the TIMER (Rho =0.438; P=8.44e–03) method; and activated mast cells according to the CIBERSORT-ABS (Rho =0.357; P=3.51e–02) method. Meanwhile, *IL23R* expression was negatively associated with following immune cell types: MDSCs, according to the TIDE (Rho =–0.528; P=1.11e–03) method; neutrophils, according to the CIBERSORT (Rho =–0.396; P=1.86e–02) and CIBERSORT-ABS (Rho =–0.377; P=2.58e–02) methods; and $CD4^+$ central memory T cells, according to the XCELL (Rho =–0.339; P=4.65e–02) method (*Figure 4C*) (35-37).

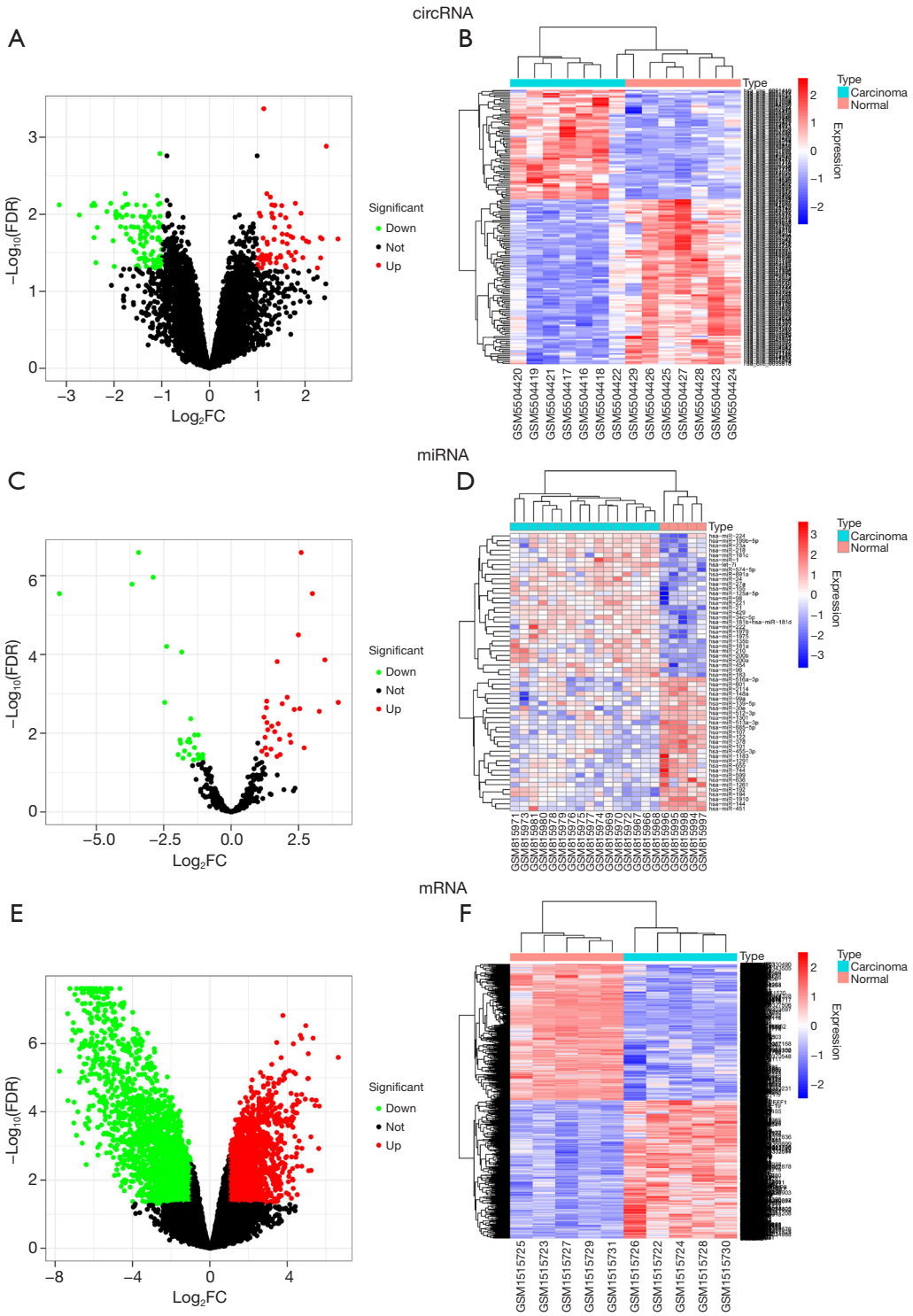

Figure 2 Identification of DEcircRNA, DEmiRNA, and DEmRNA. (A,B) The volcano plot and heatmap of circRNAs from the GSE181523 dataset, consisting of 173 DEcircRNAs. (C,D) The volcano plot and heatmap of miRNAs from the GSE32957 dataset, consisting of 58 DEmiRNAs. (E,F) The volcano plot and heatmap of mRNAs from GSE61850 dataset, consisting of 4,437 DEmRNAs. Down: downregulation with significance; Not: no significant; Up: upregulation with significance. FDR, false discovery rate; FC, fold change; DE, differentially expressed; circRNA, circular RNA; miRNA, microRNA; mRNA, messenger RNA.

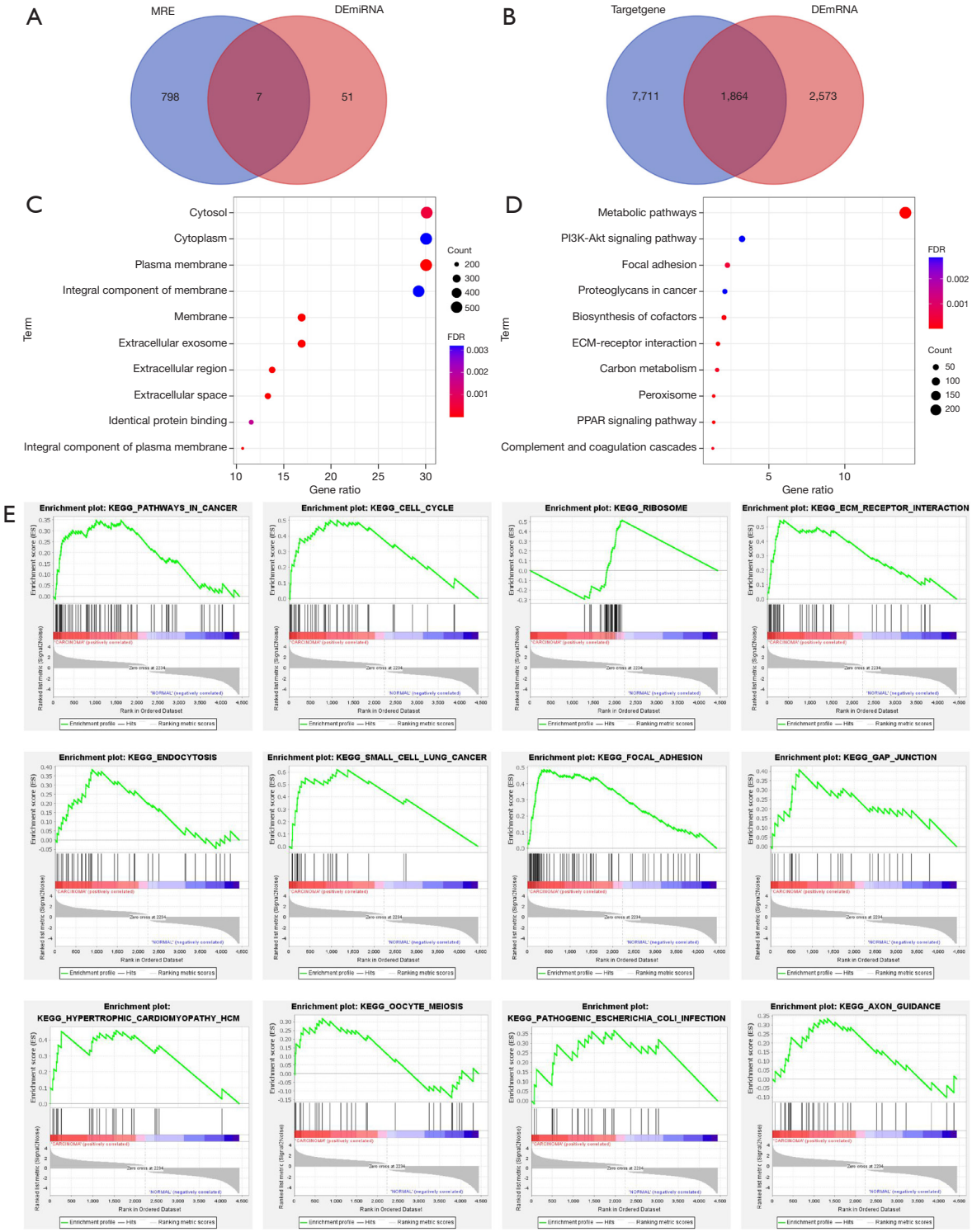

Figure 3 Functional enrichment analysis of targeted DEmRNAs. (A) Venn diagram of 7 miRNAs that were both miRNA response elements and DEmiRNAs. (B) Venn diagram of 1,864 mRNAs that were both target genes and DEmRNAs. (C) Bubble plot of the top 10 most enriched Gene Ontology terms. (D) Bubble plot of the top 10 most enriched KEGG terms. (E) Verification of the functional enrichment of targeted DEmRNAs via GSEA software. MRE, miRNA response element; DE, differentially expressed; miRNA, microRNA; mRNA, messenger RNA; targetgene, target gene; FDR, false discovery rate; PI3K, phosphoinositide 3-kinase; Akt, serine/threonine kinase; ECM, extracellular matrix; PPAR, peroxisome proliferator activated receptor; KEGG, Kyoto Encyclopedia of Genes and Genomes; HCM, hypertrophic cardiomyopathy; GSEA, Gene Set Enrichment Analysis.

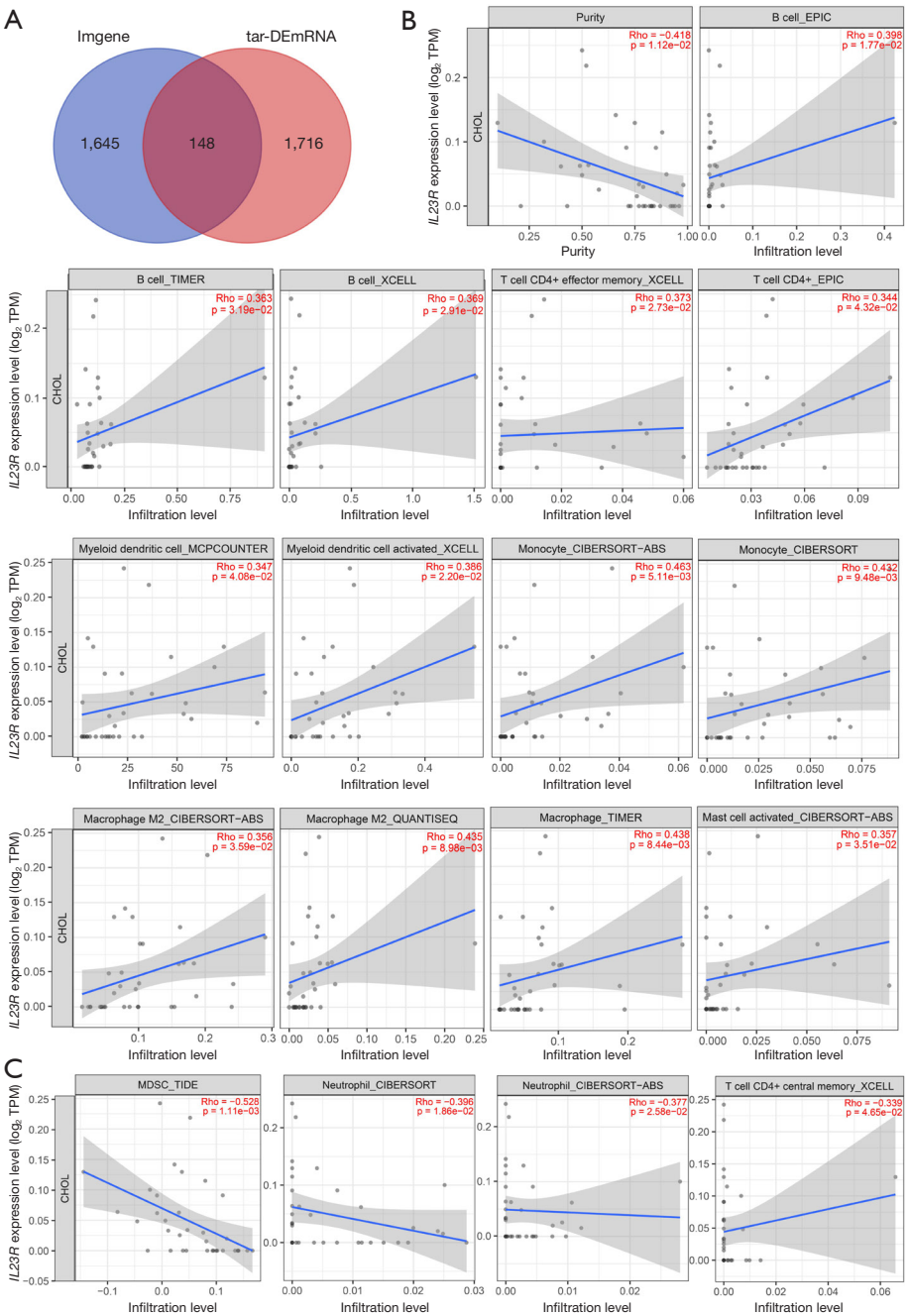

Figure 4 *IL23R* was related to CHOL immune infiltration abundance. (A) Venn diagram of mRNAs that both targeted differentially expressed mRNAs and immune-related genes. (B) The expression of *IL23R* in CHOL was negatively correlated with the proportion of tumor cells. *IL23R* expression had a positive correlation with B cells according to the EPIC, TIMER, and XCELL methods; $CD4^+$ effector memory T cells according to the XCELL method; $CD4^+$ T cells according to the EPIC method; myeloid DCs according to the MCPCOUNTER method; activated myeloid DCs according to the XCELL method; monocytes according to the CIBERSORT-ABS and CIBERSORT methods; M2 macrophages according to the CIBERSORT-ABS and QUANTISEQ methods; macrophages according to the TIMER method; and activated mast cells according to the CIBERSORT-ABS method. (C) *IL23R* expression was negatively associated with MDSC according to the TIDE method, neutrophils according to the CIBERSORT and CIBERSORT-ABS methods, and $CD4^+$ central memory T cells according to the XCELL method. According to the on the TIMER2.0 database, there was no linear relationship between the infiltration level of $CD4^+$ central memory T cells and the expression of *IL23R*, which led to the inconsistency between the slope of the line and the Rho value. (B,C) were downloaded from TIMER2.0 database, and no permission was needed. imgene, immune-related gene; tar-DEmRNA, the intersection mRNA of miRNA target gene and DEmRNA; DE, differentially expressed; mRNA, messenger RNA; miRNA, microRNA; *IL23R*, interleukin 23 receptor; TPM, transcripts per million; CHOL, intrahepatic cholangiocarcinoma; DCs, dendritic cells; MDSC, myeloid-derived suppressor cell.

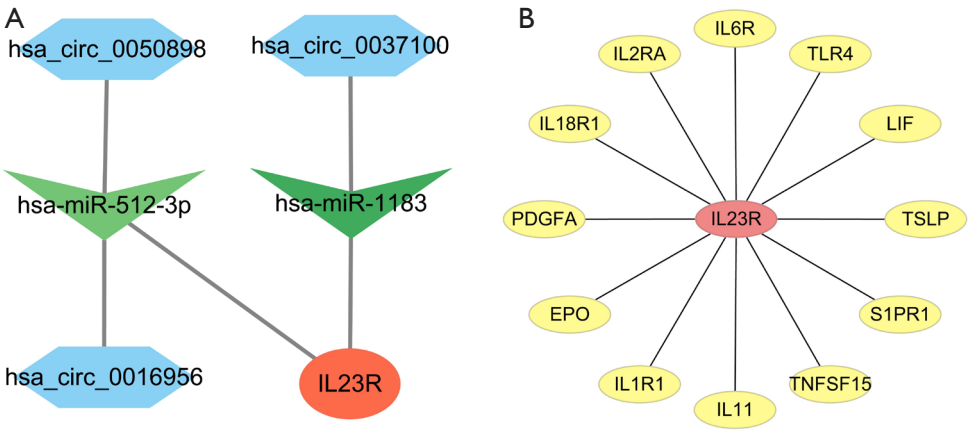

Figure 5 Construction of the circRNA-miRNA-*IL23R* and protein-protein interaction network of *IL23R*. (A) Interactions of circRNA-miRNA-*IL23R*. The blue patterns represent circRNA, the green patterns represent miRNA, and the red patterns represent mRNA. (B) Protein-protein interaction network between *IL23R* and the other directly related mRNAs. *IL23R*, interleukin 23 receptor; circRNA, circular RNA; miRNA, microRNA; mRNA, messenger RNA.

Construction of circRNA-miRNA-IL23R and protein-protein interaction networks for IL23R

MREs were identified using the CircBank database, and the target genes of miRNA were obtained using Targetscan. Through intersection, the miRNAs corresponding to the target gene of *IL23R*, namely hsa-miR-512-3p and hsa-miR-1183, were identified, as were the relevant circRNAs corresponding to the MREs of hsa-miR-512-3p and hsa-miR-1183. The circRNA-miRNA-mRNA interactions were integrated (*Figure 5A*) using Cytoscape, which provided the links among the circRNAs (hsa_circ_0050898, hsa_circ_0037100, and hsa_circ_0016956), the miRNAs (hsa-miR-512-3p, and hsa-miR-1183), and *IL23R*. Removing the unconnected nodes, we analyzed the 148-im-tar-DEmRNA PPI network using the Search Tool for the Retrieval of Interacting Protein (STRING; https://cn.string-db.org/cgi/input?sessionId=bcgnSYBYHI9T&input_page_active_form=multiple_identifiers; RRID: SCR_005223) website. *Figure 5B* shows the protein network directly related to *IL23R*, while the other PPI networks are shown in the online table (available at https://cdn.amegroups.cn/static/public/10.21037tcr-23-455-7.pdf).

A low expression of IL23R was associated with poor prognosis in CHOL

The GEPIA database and DriverDBv3 database were used to perform prognostic analysis. As the cutoff value was set to the median in the GEPIA database, the OS [hazard ratio (HR) =0.19; P=0.0042] (*Figure 6A*) and the DFS (HR =0.22; P=0.0052) (*Figure 6B*) of patients with CHOL and low *IL23R* expression were lower than those with a high expression of *IL23R* (33). In the DriverDBv3 database (32), the OS (HR =0.273; P=0.00956) (*Figure 6C*) and the disease-free interval (DFI) (HR =0.245; P=0.0285) (*Figure 6D*) of patients with CHOL and a low *IL23R* expression were lower than those of patients with a high expression of *IL23R* when the cutoff value was the median. The progression-free interval (PFI) (HR =0.298; P=0.00838) (*Figure 6E*) and the disease-specific survival (DSS) (HR =0.312; P=0.0254) (*Figure 6F*) of a low *IL23R* expression were also low in the DriverDBv3 database with the cutoff value equal to the median. With the cutoff values set as the mean value, the OS (HR =0.184; P=0.0118) (*Figure 6G*), PFI (HR =0.0985; P=0.000261) (*Figure 6H*), and DSS (HR =0.175; P=0.0564) (*Figure 6I*) of patients with CHOL and a low expression of *IL23R* were consistent results with those from the DriverDBv3 database. The specific information concerning the relationship of *IL23R* with CHOL progression is shown in the online table (available at https://cdn.amegroups.cn/static/public/10.21037tcr-23-455-8.pdf). In addition, to verify the relationship between *IL23R* expression and the prognosis of patients, the data of OS and DFS in patients with CHOL from TCGA were obtained via the UCSC Xena website. As shown in the *Figure 6J* and *Figure 6K*, the OS (P=0.0348) and PFI (P=0.0294) of patients with CHOL and a low expression of *IL23R* were shorter, which

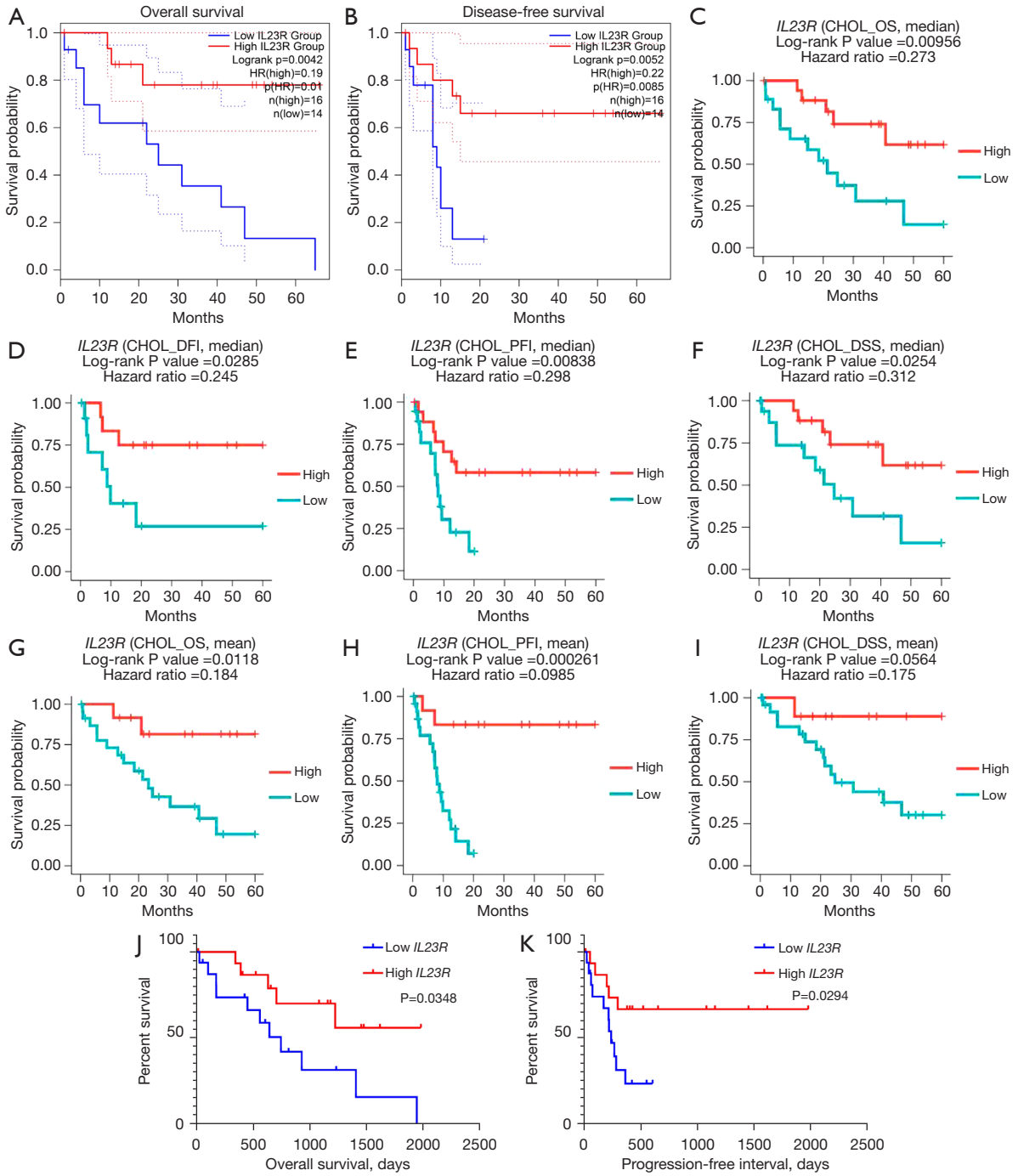

Figure 6 Low expression of *IL23R* was associated with poor prognosis in CHOL. (A) The OS (HR =0.19, P=0.0042) and (B) the disease-free survival (HR =0.22; P=0.0052) in patients with CHOL and high or low *IL23R* expression (GEPIA, cutoff value: median). (C) The OS (HR =0.273; P=0.00956), (D) the DFI (HR =0.245; P=0.0285), (E) the PFI (HR =0.298, P=0.00838), and (F) the DSS (HR =0.312, P=0.0254) in patients with CHOL with high or low *IL23R* expression (DriverDBv3, cutoff value: median). (G) The OS (HR =0.184, P=0.0118), (H) the PFI (HR =0.0985; P=0.000261), and (I) the DSS (HR =0.175; P=0.0564) in patients with CHOL with a high or low *IL23R* expression (DriverDBv3, cut-off value: mean). Verification of the relationship between *IL23R* expression and (J) the OS (P=0.0348) and (K) the PFI (P=0.0294) of patients with CHOL in TCGA obtained from the UCSC Xena website. (A,B) are downloaded from the GEPIA database. (C-I) are downloaded from the DriverDBv3 database. Permission for use of these figures is not required. *IL23R*, interleukin 23 receptor; HR, hazard ratio; CHOL, intrahepatic cholangiocarcinoma; OS, overall survival; DFI, disease-free interval; PFI, progression-free interval; DSS, disease-specific survival; GEPIA, Gene Expression Profiling Interactive Analysis.

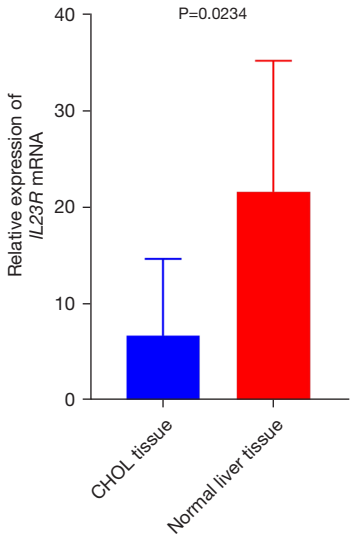

Figure 7 *IL23R* had a low expression in CHOL. The expression of *IL23R* in CHOL tissue was lower than that in healthy liver tissue performed according to RT-qPCR. *IL23R*, interleukin 23 receptor; mRNA, messenger RNA; CHOL, intrahepatic cholangiocarcinoma; RT-qPCR, real-time quantitative polymerase chain reaction.

confirmed the results from the GEPIA database and DriverDBv3 database.

Verification of IL23R expression level in CHOL

RT-qPCR was performed to explore the expression level of *IL23R* in CHOL, and the *IL23R* RNA expression in CHOL tissue was found to be lower than that in healthy liver tissue (*Figure* 7).

Discussion

CHOL is difficult to diagnose and differentiate (38), and compared to patients with other types of CCA, those with CHOL have a worse prognosis, as indicated by lower OS and cancer-specific survival rates (39). Patients with CHOL often have no symptoms at the early stage, with 70% of the patients having advanced or metastatic tumors at the time of diagnosis (5). By this time, the chance of survival for patients has declined, and there is no satisfactory treatment (40). Presently, immunotherapy is in an emerging stage of development and can also be applied in CHOL (41). However, the research on the prognosis of patients with CHOL remains still inadequate, and there is thus an urgent need to identify relevant biomarkers to improve the treatment of patients with CHOL.

In this study, the abnormal expression of circRNA, miRNA, and mRNA in CHOL was confirmed via bioinformatics analysis, with *IL23R* showing a low expression in CHOL. GO and KEGG functional enrichment analyses, verified by GSEA software, showed that DEmRNA in CHOL is related to cytosol, plasma membrane, cytoplasm, integral component of membrane, extracellular exosome, metabolic pathways, pathways in cancer, PI3K-Akt signaling pathway, human papillomavirus infection, and focal adhesion, among other aspects. The overexpression of *IL23R* via RAS/mitogen-activated protein kinase and STAT3 pathways has been proven to induce apoptosis in 293ET and HeLa cells but does not inhibit STAT1 or PI3K-Akt signaling pathways (42). There is little research on *IL23R* in cancer nowadays. Nevertheless, leucine zipper ATF-like transcription factor (Batf) was found to be coexpressed with *IL23R* in infiltrating $CD4^+$ T cells of colon cancer, while Batf-dependent *IL23R*$^+$IL-6^+CD4^+Th17 cells were shown to control the formation of IL-23-driven colitis-related tumors and the progression of sporadic colon tumors. Batf-dependent *IL23R*$^+$T cells might be a potential therapeutic target to limit the progression of colon cancer (43). At present, little is known concerning the functional mechanism of *IL23R* in the development of CHOL. However, it was reported that IL-23 produced by macrophages derived from liver monocytes plays a major role in the pathogenesis of primary biliary cirrhosis (44), which is one of the main risk factors of CHOL (45). These and similar findings point to productive research directions in CHOL, especially related to the PI3K-Akt signaling pathway, immune-related TME, and amino acid metabolism.

Cytokines are one of the components of the TME. IL-23 is a covalently linked heterodimeric hematopoietic cytokine, which is produced by activated DCs and macrophages (46). *IL23R* is a subunit of IL23A/IL-23 receptor, which is a newly discovered member of the hemopoietic receptor superfamily. It is encoded by a gene located within 150 kb of the human chromosome 1 *IL12Rβ2* gene (47). Recent research demonstrated that antibody-mediated blockade of *IL23R* can augment the instability of intratumoral T cells and enhance immunotherapy. It was further found that blocking the expression of *IL23R* could increase the expression of IL-12 and interferon-γ in Tregs, leading to the recruitment of $CD8^+$ T cells and further destabilizing Tregs, thus inhibiting the development of tumor (10). In

another study, the proportion of interferon-γ-producing NK cells in the lungs from B16F10 tumor-bearing mice increased the inhibition of experimental lung metastasis, with the antibody blocking *IL23R* being more effective than the antibody neutralizing IL-23 (48). According to the bioinformatics analysis mentioned in our study, *IL23R* was related to the immune infiltration of CHOL cells. *IL23R* expression had a positive correlation with some immune infiltration-related cells, including $CD4^+$ effector memory T cells and $CD4^+$ T cells, and a negative associated with others, including $CD4^+$ central memory T cells. Zhan *et al.* found that IL-23/IL-17A signaling pathway was closely related to chronic inflammation of the bile duct in primary biliary cirrhosis and the functional loss of Tregs, which led to the decrease of Foxp3 expression and mediated the tolerance loss of primary biliary cirrhosis (49). In addition, a recent study revealed that patients with CHOL and a high proportion of $Foxp3^+$ Tregs in mesenchymal tissue had a longer relapse-free survival (50). According to Shi *et al.*, CD4CD161 cells from patients with primary biliary cirrhosis have a higher expression of IL-17 after being stimulated with IL-23 and IL-1β (51). Therefore, as primary biliary cirrhosis is related to CHOL, the expression of *IL23R* in CHOL may exert a certain role in TME, thus affecting the immune efficacy.

As posttranscriptional regulators, circRNAs are formed by splicing exons head to tail (52). As non-coding RNAs, only a few circRNAs have been confirmed to regulate biological processes such as cell proliferation, migration, or invasion. The biological functions of circRNAs can be achieved by acting as miRNA or protein "sponges", by regulating protein function, or by self-translation (53). Therefore, further research into circRNAs is particularly critical. In this study, we identified 69 upregulated and 104 downregulated circRNAs and 805s MRE in CHOL. In addition, 3 circRNAs (hsa_circ_0050898, hsa_circ_0037100, and hsa_circ_0016956) and 2 miRNAs (hsa-miR-512-3p and hsa-miR-1183) were integrated to form circRNA-miRNA-mRNA interactions with *IL23R*. Chen *et al.* found that hsa_circ_0050898 can promote the proliferation and metastasis of CHOL by acting as a molecular sponge of miR-424-5p and by activating FZD7 through interaction with YBX1 (21). Moreover, Wang *et al.* reported that USF2-mediated hsa_circ_0050898 might promote the occurrence and development of breast cancer and could thus serve as a novel target for the diagnosis and treatment of breast cancer (54). Furthermore, Mohamadzade *et al.* demonstrated hsa-miR-512-3p to be a cell-type-specific tumor inhibitor that can act as a potential biomarker for breast cancer diagnosis (55). However, little research has been conducted concerning the role of circRNA-miRNA-mRNA of *IL23R* in CHOL. Our findings suggest the possible existence of a ceRNA network of *IL23R* in CHOL, but more experimental studies need to be performed to verify the possible pathways.

As a positive regulator in the initiation of T helper cells, *IL23R* is considered to be the principal coordinator of inflammation-driven tumors (56). However, the role of *IL23R* in cancer is not completely clear. In studies of laryngeal cancer, bladder cancer, and non-small cell lung cancer (NSCLC), a high expression of *IL23R* has been associated with poor prognosis (9,12,57). A different study found EIF5A2 to be an independent prognostic indicator for CHOL. High levels of EIF5A2 can activate the PI3K/Akt/mTOR signaling pathway, thus promoting the proliferation, migration, and invasion of CHOL cells (58). Moreover, brusatol can inhibit CHOL cell proliferation and the epithelial-mesenchymal transition process through PI3K-Akt pathway and thus promote tumor cell apoptosis, providing a direction for CHOL therapy (59). It has recently been shown that a higher baseline level of IL-23 can improve the clinical results of atezolizumab combined with cobimetinib in the treatment of advanced biliary tract cancers (16). However, the prognosis value of *IL23R* in patients with CHOL is still unclear. Through bioinformatics analysis, we found that a low expression of *IL23R* was related to the poor prognosis of CHOL, which seems to be consistent with the improvement of clinical outcomes in patients with advanced biliary tract cancers treated with atezolizumab combined with cobimetinib with a high baseline level of IL-23. Additionally, the GEPIA and DriverDBv3 databases showed that patients with CHOL and a low expression of *IL23R* had a lower OS and DFS. However, further research is needed to determine how *IL23R* affects the prognosis of patients with CHOL and clarify the detailed mechanism of *IL23R* in this relationship.

Conclusions

This is the first study to analyze the relationship between *IL23R* expression in CHOL and total survival time. The low expression of *IL23R* resulted in the decreased survival time of patients with CHOL. *IL23R* can be considered a potential biomarker for the diagnosis and treatment of patients with CHOL. However, most of the results in this study were obtained via bioinformatics analysis. In the future, a series of experiments should be conducted

to further verify the role of *IL23R* in the diagnosis or prognosis of CHOL and determine whether interfering with *IL23R* expression can aid in tumor treatment.

Acknowledgments

The image elements in *Figure 1* were obtained from Vecteezx (https://www.vecteezy.com/) and SMART SERVIER (https://smart.servier.com/).
Funding: This work was supported by Shenzhen Science and Technology Innovation Commission Project (Nos. JCYJ20190809100005672, ZDSYS20190902092855097, and KCXFZ20200201101050887), the General Program (No. JCYJ20210324105609024), and the Shenzhen Sanming Project (No. SZSM201612041).

Footnote

Reporting Checklist: The authors have completed the TRIPOD reporting checklist. Available at https://tcr.amegroups.com/article/view/10.21037/tcr-23-455/rc

Peer Review File: Available at https://tcr.amegroups.com/article/view/10.21037/tcr-23-455/prf

Conflicts of Interest: All authors have completed the ICMJE uniform disclosure form (available at https://tcr.amegroups.com/article/view/10.21037/tcr-23-455/coif). The authors have no conflicts of interest to declare.

Ethical Statement: The authors are accountable for all aspects of the work in ensuring that questions related to the accuracy or integrity of any part of the work are appropriately investigated and resolved. This study was conducted in accordance with the Declaration of Helsinki (as revised in 2013) and was approved by Ethics Committee of Guangdong Provincial People's Hospital (No. KY-Q-2022-321-01). Written informed consent for participation was not required for this study in accordance with the national legislation and the institutional requirements.

References

1. Banales JM, Cardinale V, Carpino G, et al. Expert consensus document: Cholangiocarcinoma: current knowledge and future perspectives consensus statement from the European Network for the Study of Cholangiocarcinoma (ENS-CCA). Nat Rev Gastroenterol Hepatol 2016;13:261-80.
2. Zhang H, Yang T, Wu M, et al. Intrahepatic cholangiocarcinoma: Epidemiology, risk factors, diagnosis and surgical management. Cancer Lett 2016;379:198-205.
3. Blechacz B, Komuta M, Roskams T, et al. Clinical diagnosis and staging of cholangiocarcinoma. Nat Rev Gastroenterol Hepatol 2011;8:512-22.
4. Sung H, Ferlay J, Siegel RL, et al. Global Cancer Statistics 2020: GLOBOCAN Estimates of Incidence and Mortality Worldwide for 36 Cancers in 185 Countries. CA Cancer J Clin 2021;71:209-49.
5. Banales JM, Marin JJG, Lamarca A, et al. Cholangiocarcinoma 2020: the next horizon in mechanisms and management. Nat Rev Gastroenterol Hepatol 2020;17:557-88.
6. Beal EW, Tumin D, Moris D, et al. Cohort contributions to trends in the incidence and mortality of intrahepatic cholangiocarcinoma. Hepatobiliary Surg Nutr 2018;7:270-6.
7. Teng MW, Bowman EP, McElwee JJ, et al. IL-12 and IL-23 cytokines: from discovery to targeted therapies for immune-mediated inflammatory diseases. Nat Med 2015;21:719-29.
8. Li W, An N, Wang M, et al. Interleukin-23 receptor defines T helper 1-like regulatory T cells in oral squamous cell carcinoma. Immun Inflamm Dis 2022;10:e746.
9. Tao Y, Shen H, Liu Y, et al. IL-23R in laryngeal cancer: a cancer immunoediting process that facilitates tumor cell proliferation and results in cisplatin resistance. Carcinogenesis 2021;42:118-26.
10. Wight AE, Sido JM, Degryse S, et al. Antibody-mediated blockade of the IL23 receptor destabilizes intratumoral regulatory T cells and enhances immunotherapy. Proc Natl Acad Sci U S A 2022;119:e2200757119.
11. Xu X, Yang C, Chen J, et al. Interleukin-23 promotes the migration and invasion of gastric cancer cells by inducing epithelial-to-mesenchymal transition via the STAT3 pathway. Biochem Biophys Res Commun 2018;499:273-8.

12. Liu D, Xing S, Wang W, et al. Prognostic value of serum soluble interleukin-23 receptor and related T-helper 17 cell cytokines in non-small cell lung carcinoma. Cancer Sci 2020;111:1093-102.
13. Zhang T, Yu L, Shao M, et al. Associations between IL-23R gene polymorphism (rs10889677 A/C) and ankylosing spondylitis and rheumatoid arthritis susceptibility: A meta-analysis with trial sequential analysis. Autoimmunity 2022;55:388-97.
14. Kutwin M, Migdalska-Sęk M, Brzeziańska-Lasota E, et al. An Analysis of IL-10, IL-17A, IL-17RA, IL-23A and IL-23R Expression and Their Correlation with Clinical Course in Patients with Psoriasis. J Clin Med 2021;10:5834.
15. Quiroz-Cruz S, Posada-Reyes B, Alatorre-García T, et al. Genetic polymorphisms present in IL10, IL23R, NOD2, and ATG16L1 associated with susceptibility to inflammatory bowel disease in Mexican population. Eur J Gastroenterol Hepatol 2020;32:10-6.
16. Ruggieri AN, Yarchoan M, Goyal S, et al. Combined MEK/PD-L1 Inhibition Alters Peripheral Cytokines and Lymphocyte Populations Correlating with Improved Clinical Outcomes in Advanced Biliary Tract Cancer. Clin Cancer Res 2022;28:4336-45.
17. Wilusz JE, Sharp PA. Molecular biology. A circuitous route to noncoding RNA. Science 2013;340:440-1.
18. Yang L, Fu J, Zhou Y. Circular RNAs and Their Emerging Roles in Immune Regulation. Front Immunol 2018;9:2977.
19. Tang J, Wang R, Tang R, et al. CircRTN4IP1 regulates the malignant progression of intrahepatic cholangiocarcinoma by sponging miR-541-5p to induce HIF1A production. Pathol Res Pract 2022;230:153732.
20. Xu YP, Dong ZN, Wang SW, et al. circHMGCS1-016 reshapes immune environment by sponging miR-1236-3p to regulate CD73 and GAL-8 expression in intrahepatic cholangiocarcinoma. J Exp Clin Cancer Res 2021;40:290.
21. Chen Q, Wang H, Li Z, et al. Circular RNA ACTN4 promotes intrahepatic cholangiocarcinoma progression by recruiting YBX1 to initiate FZD7 transcription. J Hepatol 2022;76:135-47.
22. Liu M, Wang Q, Shen J, et al. Circbank: a comprehensive database for circRNA with standard nomenclature. RNA Biol 2019;16:899-905.
23. McGeary SE, Lin KS, Shi CY, et al. The biochemical basis of microRNA targeting efficacy. Science 2019;366:eaav1741.
24. Ashburner M, Ball CA, Blake JA, et al. Gene ontology: tool for the unification of biology. The Gene Ontology Consortium. Nat Genet 2000;25:25-9.
25. Kanehisa M, Sato Y, Kawashima M, et al. KEGG as a reference resource for gene and protein annotation. Nucleic Acids Res 2016;44:D457-62.
26. Sherman BT, Hao M, Qiu J, et al. DAVID: a web server for functional enrichment analysis and functional annotation of gene lists (2021 update). Nucleic Acids Res 2022;50:W216-21.
27. Huang da W, Sherman BT, Lempicki RA. Systematic and integrative analysis of large gene lists using DAVID bioinformatics resources. Nat Protoc 2009;4:44-57.
28. Mootha VK, Lindgren CM, Eriksson KF, et al. PGC-1alpha-responsive genes involved in oxidative phosphorylation are coordinately downregulated in human diabetes. Nat Genet 2003;34:267-73.
29. Subramanian A, Tamayo P, Mootha VK, et al. Gene set enrichment analysis: a knowledge-based approach for interpreting genome-wide expression profiles. Proc Natl Acad Sci U S A 2005;102:15545-50.
30. Liberzon A, Subramanian A, Pinchback R, et al. Molecular signatures database (MSigDB) 3.0. Bioinformatics 2011;27:1739-40.
31. Liberzon A, Birger C, Thorvaldsdóttir H, et al. The Molecular Signatures Database (MSigDB) hallmark gene set collection. Cell Syst 2015;1:417-25.
32. Liu SH, Shen PC, Chen CY, et al. DriverDBv3: a multi-omics database for cancer driver gene research. Nucleic Acids Res 2020;48:D863-70.
33. Tang Z, Li C, Kang B, et al. GEPIA: a web server for cancer and normal gene expression profiling and interactive analyses. Nucleic Acids Res 2017;45:W98-W102.
34. Bhattacharya S, Dunn P, Thomas CG, et al. ImmPort, toward repurposing of open access immunological assay data for translational and clinical research. Sci Data 2018;5:180015.
35. Li T, Fu J, Zeng Z, et al. TIMER2.0 for analysis of tumor-infiltrating immune cells. Nucleic Acids Res 2020;48:W509-14.
36. Li T, Fan J, Wang B, et al. TIMER: A Web Server for Comprehensive Analysis of Tumor-Infiltrating Immune Cells. Cancer Res 2017;77:e108-10.
37. Li B, Severson E, Pignon JC, et al. Comprehensive analyses of tumor immunity: implications for cancer immunotherapy. Genome Biol 2016;17:174.
38. Bertuccio P, Malvezzi M, Carioli G, et al. Global trends in mortality from intrahepatic and extrahepatic cholangiocarcinoma. J Hepatol 2019;71:104-14.
39. Liao P, Cao L, Chen H, et al. Analysis of metastasis

and survival between extrahepatic and intrahepatic cholangiocarcinoma: A large population-based study. Medicine (Baltimore) 2021;100:e25635.
40. Valle JW, Kelley RK, Nervi B, et al. Biliary tract cancer. Lancet 2021;397:428-44.
41. Li D, Lin S, Hong J, et al. Immunotherapy for hepatobiliary cancers: Emerging targets and translational advances. Adv Cancer Res 2022;156:415-49.
42. Shi WY, Che CY, Liu L. Human interleukin 23 receptor induces cell apoptosis in mammalian cells by intrinsic mitochondrial pathway associated with the down-regulation of RAS/mitogen-activated protein kinase and signal transducers and activators of transcription factor 3 signaling pathways. Int J Mol Sci 2013;14:24656-69.
43. Punkenburg E, Vogler T, Büttner M, et al. Batf-dependent Th17 cells critically regulate IL-23 driven colitis-associated colon cancer. Gut 2016;65:1139-50.
44. Reuveni D, Brezis MR, Brazowski E, et al. Interleukin 23 Produced by Hepatic Monocyte-Derived Macrophages Is Essential for the Development of Murine Primary Biliary Cholangitis. Front Immunol 2021;12:718841.
45. Pol JG, Paillet J, Plantureux C, et al. Beneficial autoimmunity links primary biliary cholangitis to the avoidance of cholangiocarcinoma. Oncoimmunology 2021;10:1968595.
46. Subhadarshani S, Yusuf N, Elmets CA. IL-23 and the Tumor Microenvironment. Adv Exp Med Biol 2021;1290:89-98.
47. Parham C, Chirica M, Timans J, et al. A receptor for the heterodimeric cytokine IL-23 is composed of IL-12Rbeta1 and a novel cytokine receptor subunit, IL-23R. J Immunol 2002;168:5699-708.
48. Yan J, Allen S, Vijayan D, et al. Experimental Lung Metastases in Mice Are More Effectively Inhibited by Blockade of IL23R than IL23. Cancer Immunol Res 2018;6:978-87.
49. Zhan K, Xu Y, Han M, et al. Daifan San intervenes in forkhead box P3 and the interleukin (IL)-23/IL-17A signaling pathway to help prevent and treat primary biliary cirrhosis. J Tradit Chin Med 2020;40:571-83.
50. Zheng Y, Huang N, Kuang S, et al. The clinicopathological significance and relapse predictive role of tumor microenvironment of intrahepatic cholangiocarcinoma after radical surgery. Cancer 2023;129:393-404.
51. Shi T, Zhang T, Zhang L, et al. The Distribution and the Fibrotic Role of Elevated Inflammatory Th17 Cells in Patients With Primary Biliary Cirrhosis. Medicine (Baltimore) 2015;94:e1888.
52. Memczak S, Jens M, Elefsinioti A, et al. Circular RNAs are a large class of animal RNAs with regulatory potency. Nature 2013;495:333-8.
53. Kristensen LS, Andersen MS, Stagsted LVW, et al. The biogenesis, biology and characterization of circular RNAs. Nat Rev Genet 2019;20:675-91.
54. Wang X, Xing L, Yang R, et al. The circACTN4 interacts with FUBP1 to promote tumorigenesis and progression of breast cancer by regulating the expression of proto-oncogene MYC. Mol Cancer 2021;20:91.
55. Mohamadzade Z, Mahjoubi F, Soltani BM. Introduction of hsa-miR-512-3p as a new regulator of HER2 signaling pathway in breast cancer. Breast Cancer Res Treat 2021;185:95-106.
56. El-Gedamy M, El-Khayat Z, Abol-Enein H, et al. Rs-10889677 variant in interleukin-23 receptor may contribute to creating an inflammatory milieu more susceptible to bladder tumourigenesis: report and meta-analysis. Immunogenetics 2021;73:207-26.
57. Liu J, Wang L, Wang T, et al. Expression of IL-23R and IL-17 and the pathology and prognosis of urinary bladder carcinoma. Oncol Lett 2018;16:4325-30.
58. Yang SH, Hu S, Kang Q, et al. EIF5A2 promotes proliferation and invasion of intrahepatic cholangiocarcinoma cells. Clin Res Hepatol Gastroenterol 2022;46:101991.
59. Chen Z, He B, Zhao J, et al. Brusatol suppresses the growth of intrahepatic cholangiocarcinoma by PI3K/Akt pathway. Phytomedicine 2022;104:154323.

Cite this article as: Zhang LT, Yang YF, Chen XM, Wang SB, Tong GL. *IL23R* as an indicator of immune infiltration and poor prognosis in intrahepatic cholangiocarcinoma: a bioinformatics analysis. Transl Cancer Res 2023;12(10):2461-2476. doi: 10.21037/tcr-23-455

